Geology, Geophysics & Environment 2026, vol. 52 (1): 53–68

Application of the ground penetrating radar (GPR) method in the detection of underground utilities above the Kobilja Glava Tunnel

Ekrem Bektašević[1], Satko Filipović[2], Mirnes Bojić[3], Luka Crnogorac[4], Kemal Gutić[5], Krzysztof Skrzypkowski[6]

[1] *University of Tuzla, Faculty of Mining, Geology and Civil Engineering, Tuzla, Bosnia and Herzegovina, ORCID ID: 0000-0001-6742-966X*
[2] *Road Direction of Sarajevo Canton, Ministry of Transport of Sarajevo Canton, Sarajevo, Bosnia and Herzegovina, e-mail: sat-ko.filipovic@dp.ks.gov.ba, ORCID ID: 0009-0003-7456-4773*
[3] *BN PRO d.o.o. Sarajevo, Sarajevo, Bosnia and Herzegovina, e-mail: mirnes@bnpro.ba*
[4] *University of Belgrade, Faculty of Mining and Geology, Belgrade, Serbia, e-mail: luka.crnogorac@rgf.bg.ac.rs, ORCID ID: 0000-0002-9897-270X*
[5] *University of Tuzla, Faculty of Mining, Geology and Civil Engineering, Tuzla, Bosnia and Herzegovina, e-mail: ke-mal.gutic@untz.ba, ORCID ID: 0009-0008-9107-4641*
[6] *AGH University of Krakow, Faculty of Civil Engineering and Resource Management, Krakow, Poland, e-mail: skrzypko@agh.edu.pl (corresponding author), ORCID ID: 0000-0003-0819-2345*

Received: 22 January 2026; accepted: 7 April 2026; first published online: 30 April 2026

Abstract: Accurate detection and mapping of underground utilities in complex urban environments, particularly in intensive construction zones such as tunnel sites, presents a significant engineering challenge. This paper investigates the application of ground penetrating radar (GPR) integrated with high-accuracy real-time kinematic (RTK) GNSS positioning to identify and spatially define a damaged sewer pipeline above the Kobilja Glava tunnel construction site in Sarajevo, Bosnia and Herzegovina. Non-destructive investigation was required due to the lack of reliable underground utility documentation and wastewater ingress into the tunnel during construction. The study was conducted under complex urban and geotechnical conditions, including asphalt pavement, high soil moisture, heterogeneous subsurface layers, and proximity to the tunnel. GPR surveys were performed using a dual-channel Leica DS2000 system with 250 MHz and 700 MHz antennas, combining grid-based and free-profile measurements. Spatial georeferencing was achieved with a Topcon Hiper HR RTK GNSS receiver, which provides centimeter-level positioning of identified reflectors within the national coordinate system of Bosnia and Herzegovina. Data processing and interpretation followed standard GPR procedures. Results show that the sewer pipeline was reliably identified through hyperbolic reflections, with the depth of the pipe crown ranging from 1.1 to 1.7 m. Integration of GPR and GNSS data enabled precise reconstruction of the pipeline's position and depth, supporting the design of a new pipeline and reducing construction risks. The study demonstrates the high effectiveness of the integrated GPR-GNSS approach in complex urban environments near tunnel structures. These findings suggest that the integration of GPR and GNSS technologies serves not only for object detection but also provides a critical methodological framework for real-time risk assessment during underground construction. The study demonstrates how precise spatial definition of damaged infrastructure can prevent broader geotechnical instabilities, elevating the work from a local case study to a universal model for monitoring urban infrastructure under stress.

Keywords: GPR-GNSS integration, sewer pipeline detection, electromagnetic wave velocity, hyperbolic reflections, tunnel zone

https://doi.org/10.7494/geol.2026.52.1.53 ISSN 2299-8004 | e-ISSN 2353-0790 | Wydawnictwa AGH

INTRODUCTION

Ground penetrating radar (GPR) is a non-invasive geophysical technique that enables imaging of shallow subsurface structures using electromagnetic waves (Annan 2005, Luo & Lai 2020, Rangole et al. 2024). While GPR offers high spatial resolution and rapid data acquisition, its reliability in urban environments is often challenged by subsurface heterogeneity and insufficient spatial referencing. Despite these limitations, its ability to operate without surface disruption has led to its widespread application in infrastructure projects, engineering–geological investigations, and archaeology, enabling the identification of underground objects without destructive interventions (Massarelli 2021, Rasol et al. 2022). In construction practice, this is particularly vital for detecting underground utilities, as it directly reduces the risk of damage and helps preserve the functionality of existing infrastructure (Pajewski et al. 2014, Benedetto & Pajewski 2015).

The Kobilja Glava site presents a unique engineering challenge due to the overlap of critical utility infrastructure and a tunnel route under construction. Following mechanical damage to a sewer pipeline (Ø300 mm) during excavation, uncontrolled wastewater ingress into the tunnel occurred, directly compromising the excavation stability and construction dynamics. The need for non-destructive investigation arose from the absence of underground utility cadastre data and design documentation, which prevented assessment of the damage and identification of the ingress zone.

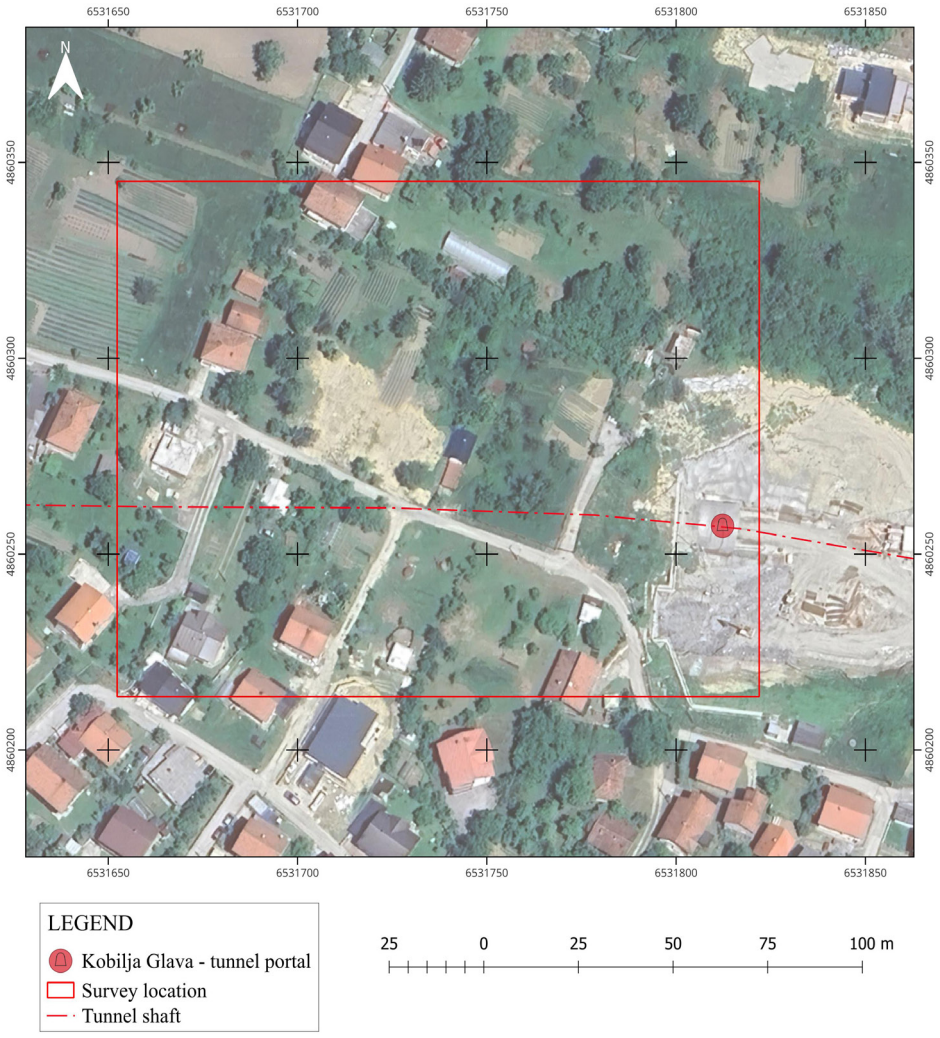

Fig. 1. *Survey location (source: Google Earth, processed by the authors)*

Previous attempts to locate the installation using conventional methods did not yield reliable results, confirming the need for advanced geophysical techniques.

The complex geotechnical and structural conditions at the site, discussed in detail in previous studies (Bektašević et al. 2024, 2025a, 2025b, 2025c, Filipović et al. 2025), further emphasized the need for a precise and reliable detection method. The surveying conditions were complicated by increased soil moisture, asphalt pavement, and the immediate proximity of the tunnel structure (WGS84: 43.886089 N, 18.383092 E), leading to signal attenuation and reduced penetration depth. Under such conditions, integration of the GPR method with high-accuracy RTK GNSS technology makes it possible not only to identify utilities but also their precise spatial georeferencing within the State Coordinate System of Bosnia and Herzegovina (DKS BiH) (Bristow & Jol 2003, Jol 2009, Catapano et al. 2019, Ghanbari et al. 2022). The application of RTK GNSS further enhances mapping reliability by enabling centimeter-level accuracy, overcoming the limitations of standalone GPR surveys (Barzaghi et al. 2016, Wang et al. 2022, ter Huurne et al. 2024, Zhang et al. 2024, Zhou et al. 2026).

The working hypothesis of this research is that an integrated GPR-GNSS approach enables centimeter-level accuracy in determining the position of shallow-buried installations under complex conditions, even in the immediate vicinity of tunnel structures. The study confirms that GPR, when combined with appropriate spatial referencing, represents a reliable tool for detecting damaged utilities, thereby contributing to risk reduction during underground construction works. The survey location, where the pipeline passes directly above the tunnel crown within a zone of minimal overburden, is shown in Figure 1. This spatial relationship, combined with saturated heterogeneous fill, required precise integration to correct for discrepancies caused by terrain slope and variations in wave propagation velocity.

MATERIALS AND METHODS

The methodological approach of the study is based on the integration of ground penetrating radar (GPR) surveying and high-accuracy satellite positioning (RTK GNSS), with the aim of reliably detecting and spatially verifying sewer installations in urban conditions above the Kobilja Glava tunnel. The broader geological setting of the research area is part of the Sarajevo-Zenica basin, specifically the Upper Miocene "Koševo series." The lithological composition at the site primarily consists of marls and fine-grained sandstones with a laminated to thin-layered texture, which are sensitive to the presence of water and can influence the dielectric properties of the soil during GPR signal propagation. This integrated approach enables simultaneous identification of subsurface reflectors and their precise georeferencing within the State Coordinate System of Bosnia and Herzegovina, thereby ensuring the immediate applicability of the results in technical documentation and spatial databases.

The methodological procedure comprised five phases: field preparation, GPR data acquisition, RTK GNSS georeferencing, office-based data processing, and reflection interpretation. The application of the GPR method is based on recording reflections of electromagnetic waves at boundaries between materials with different dielectric properties. Since the interpretation of reflector depths is directly dependent on the estimation of the electromagnetic wave propagation velocity in the ground, this study employed the standard relationship between the wave velocity and the relative dielectric permittivity of the medium (Davis & Annan 1989, Daniels 2004). This theoretical framework represents an established basis of modern GPR investigations and was applied in accordance with recommendations from relevant literature. The site conditions were characterized by asphalt pavement, natural soil, and increased moisture content, all of which affect dielectric properties and the expected electromagnetic wave velocity. The survey area is characterized by a complex geotechnical composition consisting of heterogeneous anthropogenic fill (crushed stone, clayey silt, and construction debris) overlying a degraded rock mass. At the time of the survey, the soil exhibited a high degree of saturation, as a direct consequence of the damaged sewage pipeline. This increased moisture content significantly influenced the soil's dielectric properties, leading to an increase in the relative permittivity and

a corresponding decrease in the electromagnetic wave velocity.

The GPR survey was conducted using a dual-channel Leica DS2000 system equipped with 250 MHz and 700 MHz antennas, integrated with a Topcon HiPer HR GNSS receiver. The chosen frequency combination provided a compromise between penetration depth and spatial resolution, which is particularly important in urban infrastructure surveys where shallow-buried utilities are expected (Robinson et al. 2013, Travassos et al. 2018, ImpulseRadar GPR Team 2021). The anticipated depth of the sewer pipeline was approximately 0.8–1.5 m, consistent with the penetration capabilities of the employed antennas. Under the given conditions, the expected maximum penetration depth was approximately 2–3 m for the 250 MHz antenna and about 1.0–1.5 m for the 700 MHz antenna. Georeferencing of the data obtained from GPR surveying was performed using network-based RTK GNSS positioning with a Topcon HiPer HR receiver. To achieve high precision within the national coordinate system (State Coordinate System of Bosnia and Herzegovina, DKS BiH), the FBiHPOS service was used, with correction parameters received via the NTRIP protocol. In order to ensure measurement uncertainty within centimeter-level limits, strict observation quality criteria were implemented:

- solution status: only fixed (FIX) solutions of phase ambiguities were accepted;
- geometric configuration: PDOP values were maintained below 2.0, with a minimum of 10 satellites tracked in the solution;
- signal quality: continuous monitoring was conducted to minimize the influence of multipath effects and signal obstruction, thereby ensuring the integrity of the spatial data.

This methodological approach, based on modern network correction architectures described by Sukhenko et al. (2025), enabled reliable spatial integration of GPR profiles and accurate identification of subsurface reflectors.

Field procedure of ground penetrating radar survey

The field procedure for the GPR survey was designed to ensure reliable detection of sewer installations in urban conditions characterized by pronounced infrastructural and geotechnical heterogeneity. The survey was conducted using a combination of grid (GRID) scanning and free-profile scanning, enabling the simultaneous acquisition of detailed tomographic sections and rapid verification of detected anomalies along linear routes. GRID scanning was performed on pre-defined areas above the tunnel alignment, with profiles arranged in a regular grid at 25 cm spacing, in accordance with recommendations for the resolution of linear underground objects (Jol & Bristow 2006). Three GRID sections were surveyed in this study: GRID 1 (3 m × 3 m), GRID 2 (10 m × 2.5 m), and GRID 3 (3 m × 2.5 m). A total of 356 m of GPR profiles were recorded in these areas (26 profiles in GRID 1, 52 profiles in GRID 2, and 24 profiles in GRID 3). This profile arrangement made it possible to generate reliable C-scans and a spatial correlation of reflections, which is crucial for identifying linear subsurface objects such as sewer pipelines. Free-profile scanning was used as a supplementary method in locations where terrain configuration or existing infrastructure did not allow the use of a regular grid. Profiles were guided along preliminarily identified routes and suspected zones, enabling targeted verification of anomalies detected during GRID scanning. At five locations, a total of 25 m of free-profile GPR data were collected, with one 5 m profile recorded at each site. This combined approach optimized the survey time while maintaining high detection reliability. During the fieldwork, particular attention was paid to ensuring continuous data acquisition, monitoring recording quality, and synchronizing GPR profiles with real-time GNSS positioning. This approach ensured spatial consistency of the data and allowed for their direct integration into the survey's coordinate system. To achieve this, the Topcon HiPer HR GNSS antenna was physically mounted on a dedicated vertical mast of the Leica DS2000 GPR carrier. This setup ensured a constant geometric offset between the GNSS phase center and the GPR antenna midpoint, allowing the acquisition software to automatically assign RTK-corrected coordinates to each GPR scan in real-time.

Ground penetrating radar survey parameters

The GPR survey parameters were defined based on a preliminary field inspection, the expected depth of the sewer installations, and the technical characteristics of the equipment used. The

settings were selected to ensure a stable balance between spatial resolution and penetration depth, while maintaining consistency across all recorded profiles. The survey was conducted in continuous acquisition mode, using a metric wheel to control spatial sampling. The recording time window was set to 120 ns, with 512 samples per trace, providing sufficient vertical resolution to identify shallow infrastructure objects. The spatial resolution along the profile was 4 cm. The simultaneous application of 250 MHz and 700 MHz antennas allowed for a comparative analysis of reflections, ensuring a balance between penetration depth and spatial resolution in accordance with the characteristics reported by Bakir (2017). All profiles were recorded using the same acquisition parameters, ensuring the mutual comparability of the results. Special consideration was given to the antenna's "dead zone" (near-field effects). The 700 MHz antenna was utilized to ensure high-resolution imaging of the shallow Ø300 mm pipe, while a time-zero correction was applied to all radargrams to align the first arrival with the ground surface, thereby ensuring accurate depth calibration from the zero-level. The main GPR survey parameters used in this study are summarized in Table 1.

Table 1

GPR survey parameters used in the study

Parameter	Value
System type	metric wheel
Time window	120 ns
Sampling (per trace)	512 samples
Trace interval (resolution)	4 cm
Antenna frequencies	250 MHz and 700 MHz
Calibrated velocity (v)	0.09 m/ns
Relative dielectric permittivity (ε_r)	11.1

Processing and interpretation of ground penetrating radar data

GPR data processing was performed through a combination of field and office-based processing using uNext Advanced 1.3.7 and IQMaps 15.2, following a standardized workflow aimed at improving the signal-to-noise ratio and reliably identifying reflectors relevant for infrastructure interpretation. Field processing in uNext Advanced enabled rapid verification of anomalies and preliminary depth estimation, while advanced processing in IQMaps was used to generate radargrams, tomograms, and final depth assessments. The workflow was designed to minimize subjective interpretation and ensure consistent comparability of results between individual profiles. After the initial data review and time-zero correction, procedures for background removal and frequency filtering were applied to reduce low-frequency noise and stabilize reflection amplitudes (He & Shang 2020). All profiles were subjected to a dewow filter (to remove low-frequency signal drift) and bandpass filtering aligned with the central frequencies of the antennas, further improving the signal-to-noise ratio and enhancing the interpretability of reflections. The filtering parameters were chosen to preserve the useful frequency range while minimizing artifacts in the shallow reflector zone. Amplitude gain correction (STC – smoothed gain) was applied to compensate for signal attenuation with depth, enabling clearer visualization of deeper reflectors. Depth estimation of reflectors was carried out based on hyperbolic diffraction fitting and the estimation of the electromagnetic wave propagation velocity in the medium.

The wave velocity was determined using the standard relationship between the speed of light c and the relative dielectric permittivity of the soil ε_r (Davis & Annan 1989, Daniels 2004):

$$v = \frac{c}{\sqrt{\varepsilon_r}} \tag{1}$$

After determining the wave velocity, the depth of the reflectors d was calculated using the two-way travel time t of the signal, according to the established formula (Poluha et al. 2017):

$$d = \frac{v \cdot t}{2} \tag{2}$$

The depth of the reflectors was estimated based on hyperbolic diffraction fitting across multiple representative profiles. The velocity calibration was performed using the hyperbola fitting method on clearly defined diffraction hyperbolas originating from the pipeline itself. Given the increased soil moisture due to the damaged sewer, the effective velocity was determined to be $v \approx 0.09$ m/ns, which corresponds to a relative dielectric permittivity of $\varepsilon_r \approx 11.1$. This calibrated velocity was then applied uniformly across the grid sections to ensure vertical consistency. Using

this velocity, the depth error was estimated at approximately 8–12%, which corresponds to about 10–15 cm for reflectors at depths of 1.0–1.5 m under the specific conditions. This value is consistent with expected GPR interpretation errors in urban environments and confirms the stability of depth estimates along all surveyed profiles. This approach represents standard practice in GPR interpretation and allows consistent determination of the geometry of underground objects (Daniels 2004, Jol 2009, Reynolds 2011). A final migration was applied to focus the diffraction hyperbolas and more precisely position the reflectors in the spatial domain, improving the interpretability of linear objects such as sewer pipes. For this study, Kirchhoff migration – a standard method in GPR data processing for linear infrastructure – was used. Hyperbolic diffraction fitting was performed manually, with verification across multiple profiles to reduce subjective interpretation.

The final positional accuracy of the georeferenced GPR profiles was maintained within ±2 cm horizontally and ±3 cm vertically, as verified by the internal quality reports of the RTK GNSS controller under FIX solution status, meeting the high precision requirements for the design of the new pipeline.

The operating principle of the GPR system, including the technical configuration, interaction of electromagnetic waves with subsurface structures, and signal interpretation, is illustrated in Figure 2.

Figure 2 illustrates the simplified operating principle of the GPR system, where the transmitting antenna emits an electromagnetic pulse into the ground, and the receiving antenna records the returning reflections generated at the boundaries of subsurface structures. The control unit generates the radar pulse and manages the data acquisition, while the power supply and data storage are provided by a portable field system (Goodman 1994, van der Kruk 1998). Interpretation of the sections is based on the analysis of reflections and their position relative to the tunnel alignment, enabling reliable identification of sewer installations.

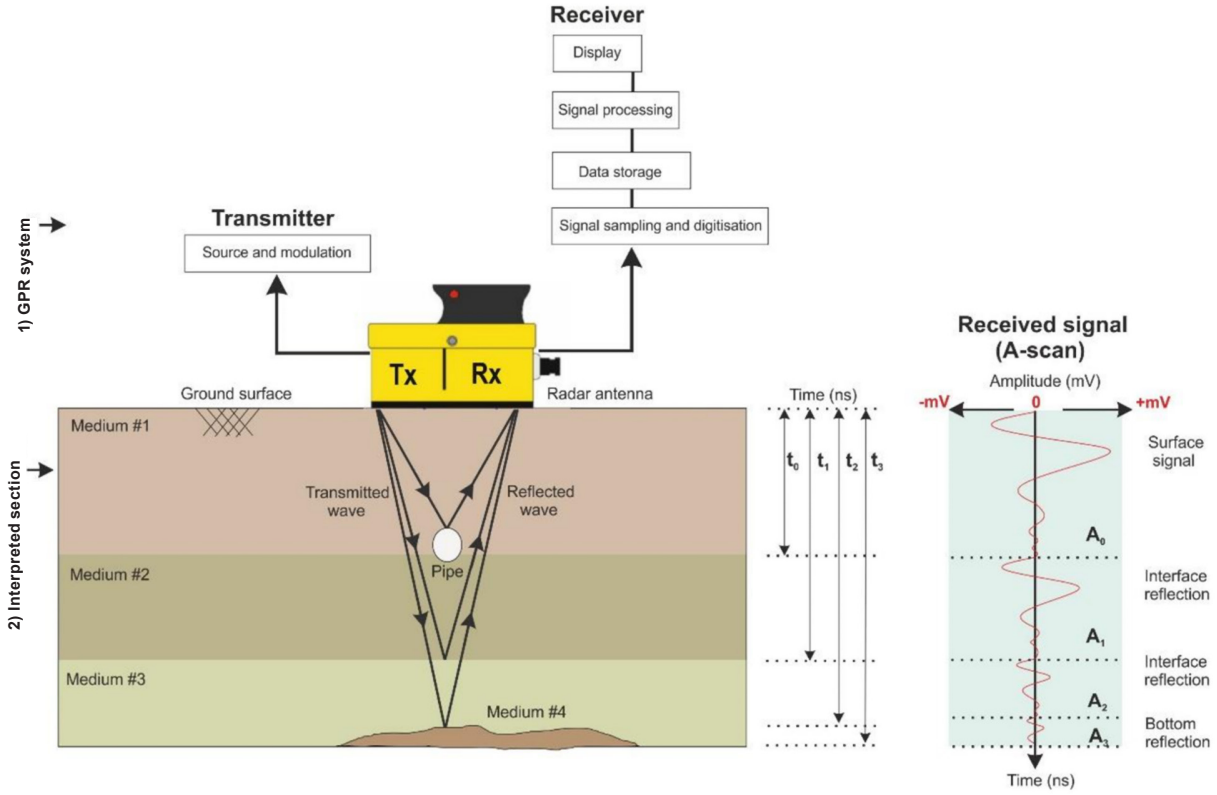

Fig. 2. *Operating principle of the GPR system: technical configuration, interaction with subsurface structures, and signal interpretation (Rasol et al. 2022)*

RESULTS

The research results are presented through the integration of GNSS measurements and GPR surveying, enabling reliable reconstruction of the position of the sewer pipeline and associated installations.

GNSS survey results

Before presenting the GPR results, it is necessary to show the spatial framework on which all detected reflectors are integrated. Figure 3 provides an overview of all GNSS points recorded during the fieldwork, which serve as the basis for the spatial integration of the GPR results. The integration was implemented by mounting the Topcon HiPer HR rover antenna directly onto the Leica DS2000 chassis using a calibrated vertical offset, enabling real-time synchronization of the GPR scan wheels with the NMEA positioning data.

The RTK GNSS system maintained a horizontal precision (s_x, s_y) of less than 1.5 cm and a vertical precision (s_z) of approximately 2.5 cm throughout the survey, ensuring that all detected reflectors are georeferenced within the official DKS BiH coordinate system with centimeter-level reliability.

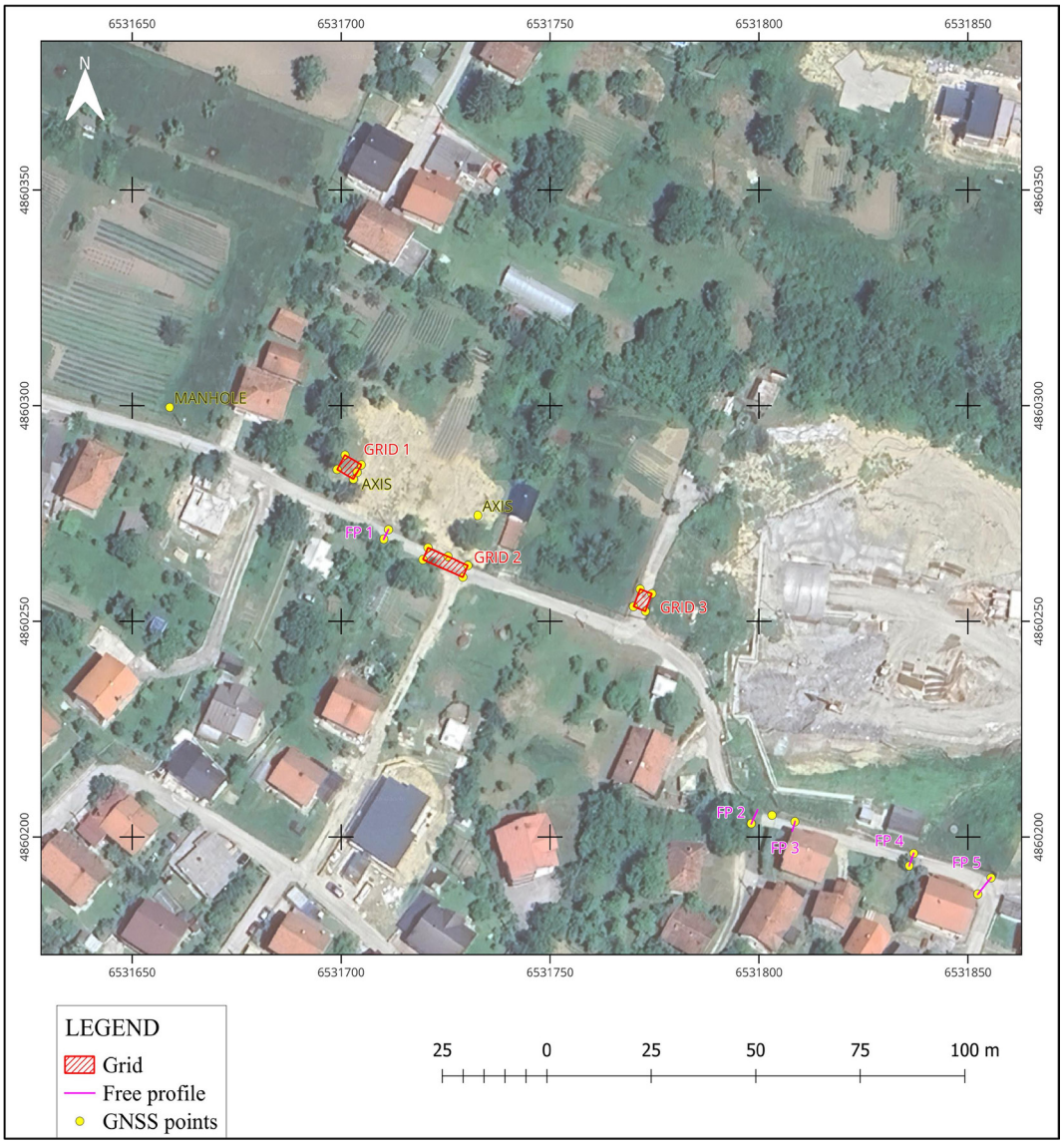

Fig. 3. *Overview of GNSS points recorded in the survey area (source: Google Earth, processed by the authors)*

GPR survey results on grid sections

GPR investigations were conducted on three spatially defined sections (GRID 1, GRID 2, and GRID 3) with the aim of identifying the sewer pipeline route and detecting any additional underground installations. Surveys were carried out using the standard GRID methodology, with parallel processing of data in the form of tomographic sections and radargrams. For clarity, only representative images are included in this study, while the remaining parts of the recorded sequences were used exclusively during the interpretation phase. Figure 4A shows the tomographic section for GRID 1, where a linear anomaly is clearly distinguishable at a depth of approximately 130–170 cm, interpreted as the sewer pipeline. Figure 4B presents the corresponding radargram, where hyperbolic reflections stand out against the background signal, further confirming the presence of the subsurface structure.

Figure 5A shows the tomographic section for GRID 2, where the primary reflections of the sewer pipeline are observed. The three red arrows in Figure 5A indicate the reconstructed longitudinal axis of the pipe and the points of maximum reflection amplitude, which were used as reference markers for spatial alignment. The recorded depths of 98 cm and 173 cm represent the top (crown) and the bottom (invert) of the pipeline structure, respectively. The vertical separation between these reflections (approximately 75 cm), which exceeds the nominal 300 mm pipe diameter, is interpreted as being a result of internal siltation and the presence of standing wastewater. This creates multiple dielectric interfaces, causing the GPR signal to reflect from both the top of the pipe and the surface of the accumulated sediment or water level at the bottom. Figure 5B presents the corresponding radargram, in which the characteristic hyperbolic reflections of the underground pipeline are clearly distinguishable.

At certain locations within GRID 2, deeper reflections were recorded that may represent the bottom of the pipe or multiple reflections caused by the dielectric contrast between the pipe and the surrounding material. Such occurrences are common in GPR surveys of underground utilities and do not affect the identification of the primary reflector. Analysis of the radargrams within GRID 2 (Fig. 5B) reveals a pronounced zone of signal attenuation directly beneath the identified pipeline hyperbolas.

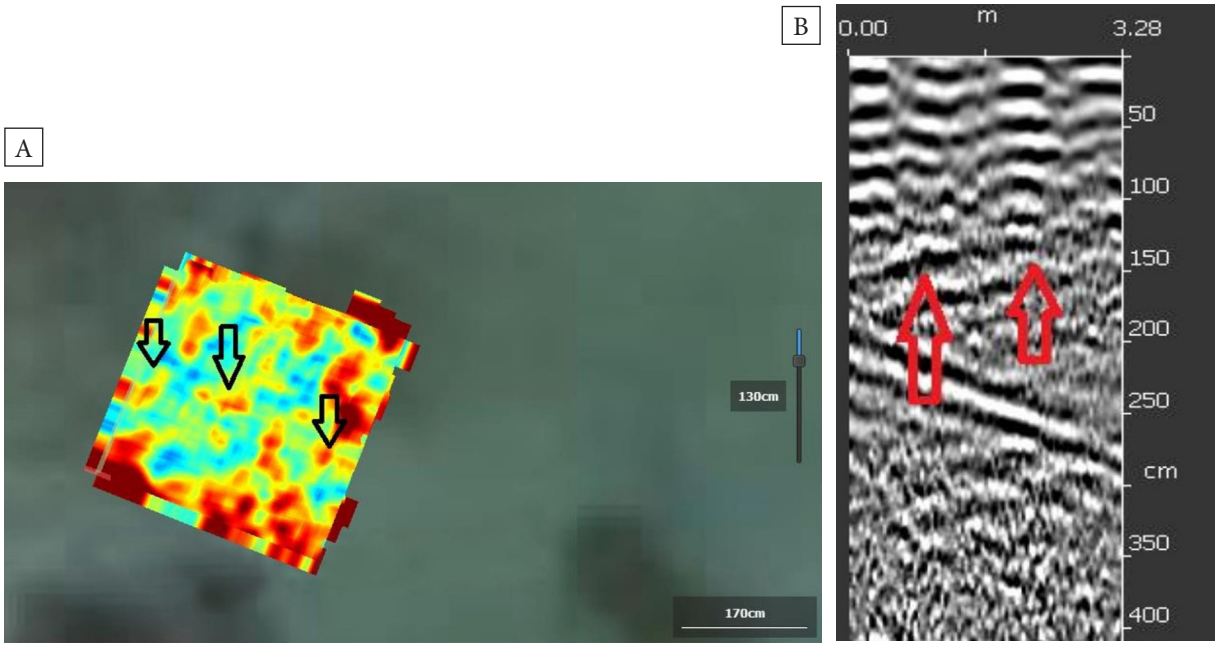

Fig. 4. *GRID 1 GPR results: A) tomographic section with pronounced linear anomaly at 130–170 cm depth; B) radargram confirming the underground installation through characteristic hyperbolic reflections*

This "shadowing" effect, characterized by a loss of coherence in deeper reflectors, serves as a diagnostic indicator of high moisture content in the circumjacent material. Such a phenomenon confirms the presence of a conductive medium – likely wastewater – that absorbs electromagnetic energy, thereby enabling the spatial localization of the leakage zone. Figure 6 shows shallow installations at a depth of approximately 22 cm, confirming the presence of additional utility pipelines along Slatina Street. The use of a high-frequency 700 MHz antenna ensured that these shallow reflections were clearly recorded outside the GPR blind zone, providing reliable detection near the surface.

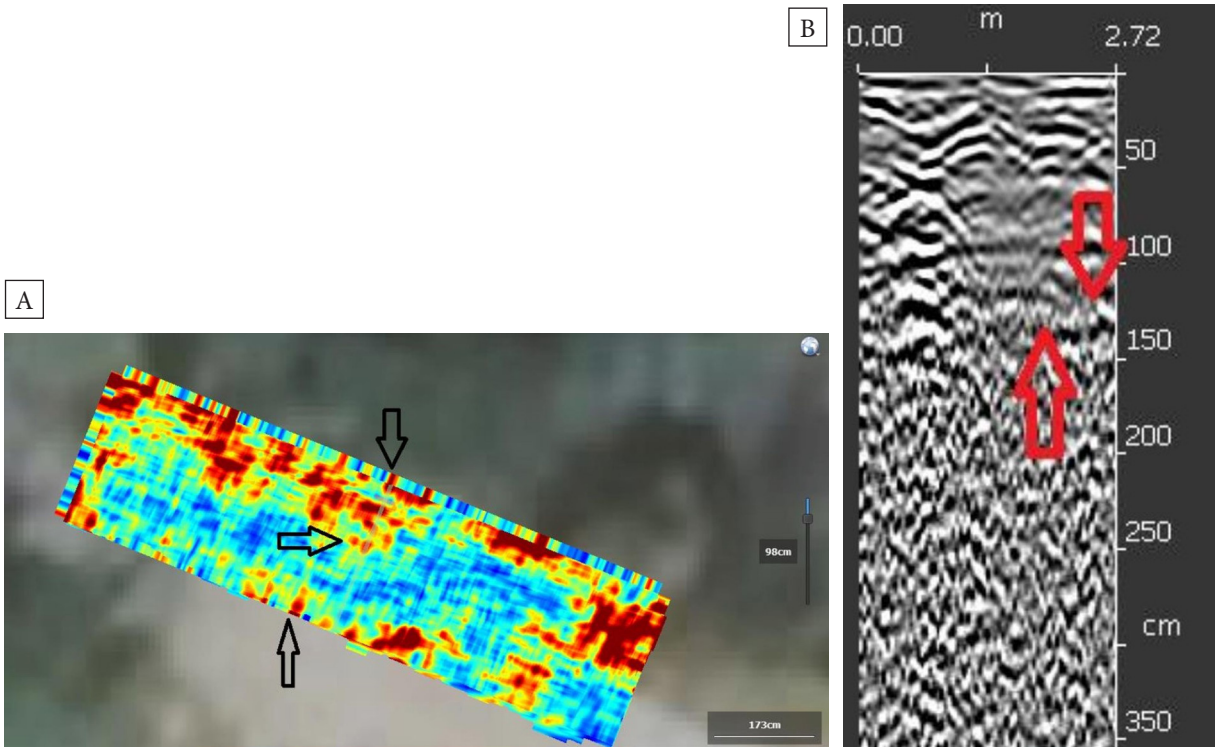

Fig. 5. *GRID 2 GPR results: A) tomographic section of pipe trajectory (arrows: boundaries and axis); B) radargram with pipe crown (98 cm) and invert (173 cm) reflections*

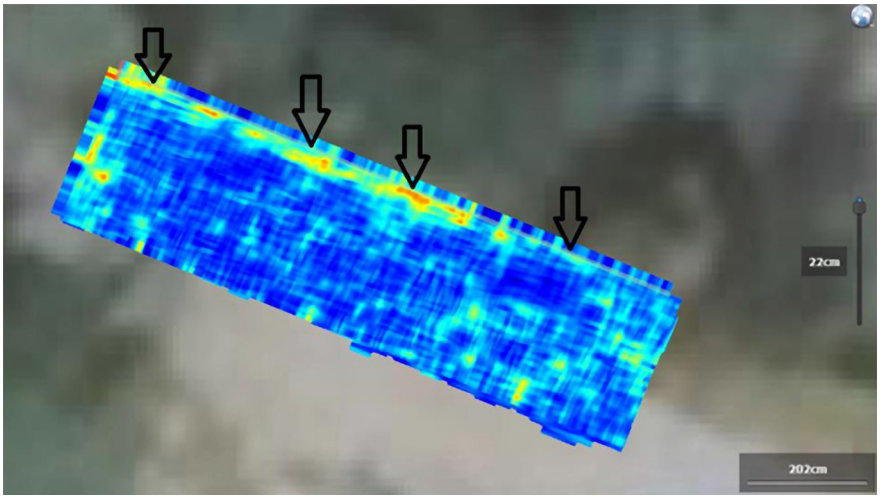

Fig. 6. *Additional installations at GRID 2 location at a depth of 22 cm*

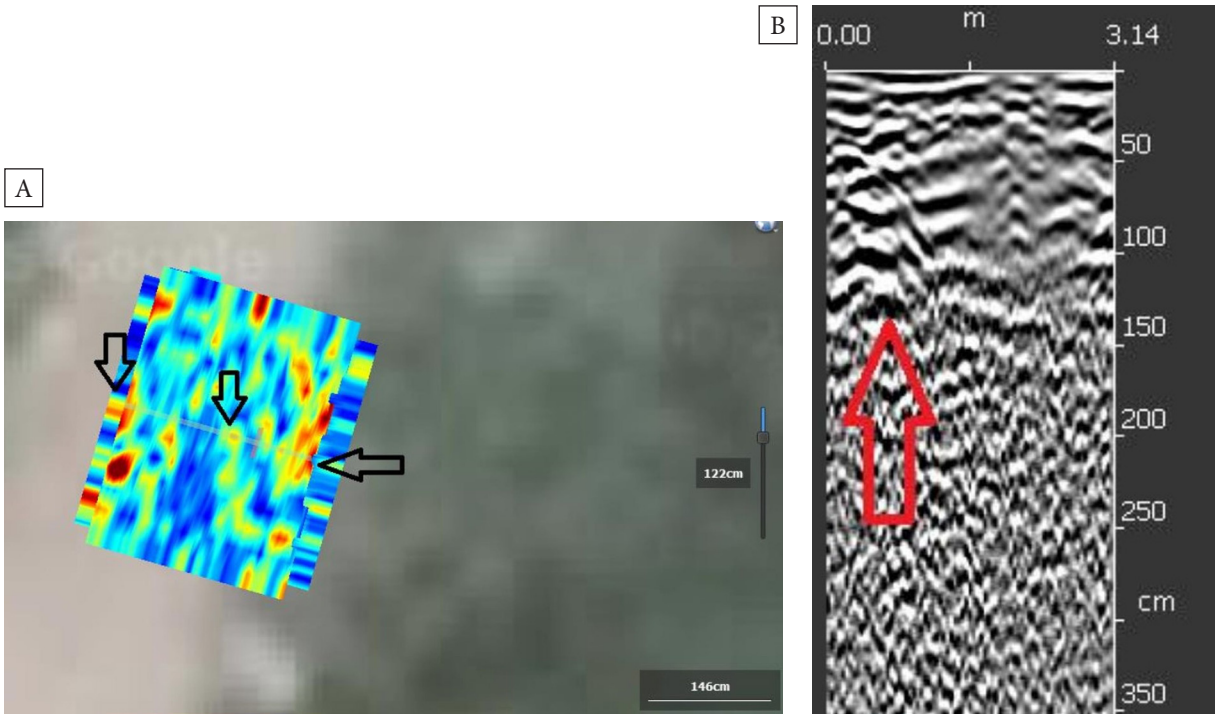

Fig. 7. *GRID 3 GPR results: A) tomographic section showing the reflection of the sewer pipeline at depths of 122–146 cm (arrows indicate the boundaries and axis of the pipeline); B) radargram clearly showing the corresponding hyperbolic reflections*

Figure 7A shows the tomographic section for GRID 3, where a reflection corresponding to the sewer pipeline is observed at depths of approximately 122–146 cm. Figure 7B presents the corresponding radargram, with clearly defined hyperbolic reflections confirming the presence of the underground installation.

Results of free profiles (FP – KanD1 to KanD7)

Free-profile surveys were conducted at multiple locations along the expected sewer pipeline route to confirm its continuity outside the GRID sections. Unlike GRID surveys, free profiles allow for rapid and flexible tracking of the pipeline route, with interpretation based on the identification of characteristic hyperbolic reflections. The free profiles enabled verification of the continuity of reflections beyond the GRID sections and confirmed that the sewer pipeline extends along the entire surveyed route without significant changes in depth. Figure 8 shows the radargram for the free profile KanD1, where a pronounced hyperbolic reflection of the sewer pipeline is clearly visible at a depth of approximately 1.35 m. It should be noted that any perceived discrepancy between the visual scale on the radargram (which may appear closer to 1.0 m) and the reported depth is due to the site-specific velocity calibration of 0.09 m/ns. While the raw radargram display often defaults to a standard soil velocity (0.1 m/ns), the analytical depth calculation accounts for the high soil permittivity ($\varepsilon_r \approx 11.1$) caused by the documented leakage, providing a more accurate representation of the physical position.

Figure 9 shows the radargram for the free profile KanD3, where the reflection occurs at a depth of approximately 1.23 m, representing a typical example of depth stability along the route. The secondary, shallower hyperbola visible at approximately 0.5 m in Figure 9 is interpreted as a minor utility line or a multiple reflection from the near-surface layers, and is not associated with the primary sewer infrastructure.

The other free profiles (KanD2 and KanD4–KanD7) exhibited similar reflection characteristics and were used in the interpretation, but are not shown in this study for brevity.

Fig. 8. *Radargram for the free profile KanD1*

Fig. 9. *Radargram for the free profile KanD3*

For clarity and quantitative comparison, Table 2 presents all detected reflection depths from the GRID sections and free profiles. It can be observed that the reflector depths range from approximately 1.09 to 1.73 m, with values on the free profiles fully consistent with the GRID survey results. This stability of depth estimates confirms the reliability of the interpretation and the continuity of the sewer pipeline along the entire surveyed area. Although Table 2 shows relatively stable depth estimates, the observed deviations of approximately 10–15 cm on certain profiles correlate with the zones of identified pipeline deformations.

Table 2
Summary of sewer pipeline reflection depths on GRID and free profiles

Location / Profile	Reflection depth [cm]	Notes
GRID 1	130; 170	linear anomaly, stable hyperbola
GRID 2	98; 173	pipe crown and invert reflections
GRID 2 – secondary reflectors	22; 202	utility (22 cm) and deep reflector (202 cm)
GRID 3	122; 146	stable reflection along the profile
FP – KanD1	135	pronounced hyperbola; depth calibrated at $v = 0.09$ m/ns
FP – KanD3	123	stable depth
FP – KanD2, KanD4–KanD7	109–135	depth range on other profiles

These variations are not due to measurement uncertainty – which remains within centimeter-level limits thanks to the high-precision RTK GNSS integration – but serve as an empirical indicator of the physical settlement of the utility line caused by the underlying tunnel excavation.

Although the results of the GPR survey demonstrated a high degree of consistency, the interpretation of reflections in urban environments is necessarily subject to certain limitations. Subsurface heterogeneity, the presence of asphalt pavement, and increased soil moisture affect the dielectric properties of the medium and can lead to local variations in electromagnetic wave propagation velocity. These variations directly impact the depth estimation of reflectors, especially in areas with layered or heterogeneous substrates. Furthermore, the presence of various utility installations and metallic elements in the heterogeneous urban substrate can generate multiple reflections and diffractions. In the context of this study, these phenomena, combined with the high dielectric contrast of the water-saturated soil, required careful signal processing and filtering to isolate the target sewer signal from the background noise and secondary hyperbolic events. Despite these limitations, the stability of reflections along both the GRID and free profiles indicates that the effects of heterogeneity were limited and did not significantly affect the reliability of the final interpretation. The obtained results have direct relevance for the design of the new sewer pipeline above the Kobilja Glava tunnel. The stability of depth values on the GRID sections and free profiles enabled a reliable reconstruction of the spatial geometry of the existing damaged pipeline, including its depth, slope, and horizontal alignment. The integration of GPR reflections with RTK GNSS measurements allowed precise georeferencing of the route within the DKS BiH system, creating conditions for the direct application of the results in the project documentation. This approach significantly reduces the risk of secondary damage during construction, allows optimization of the new pipeline route, and eliminates uncertainties arising from the lack of a cadastral record of underground installations and project documentation. Consequently, the research results represent a critical input parameter for the safe and efficient planning of rehabilitation and construction activities at the site. The stability of the depth values along GRID and free profiles further indicates that the sewer pipeline is laid in relatively uniform geotechnical conditions, without significant variations in the dielectric properties of the substrate. Such consistency of reflections further confirms the reliability of the interpretation and reduces the likelihood of misidentifying the target object. The combination of GRID surveys, free profiles, and GNSS measurements enabled a complete and reliable reconstruction of the sewer pipeline route, thereby fulfilling all the objectives of the study.

DISCUSSION

The results of this study confirm that the GPR method, when integrated with high-accuracy GNSS positioning, represents a reliable and efficient tool for detecting and spatially defining shallow sewer installations in complex urban and geotechnical conditions. Of particular significance is the stable identification of the sewer pipeline in the immediate vicinity of the tunnel structure, where pronounced electromagnetic and geotechnical disturbances are present; conditions that often limit the practical applicability of GPR methods. The measured reflection depths, ranging along the surveyed route, from approximately 1.1 to 1.7 m, indicate good consistency of interpretation and confirm that local variations in the dielectric properties of the soil had a limited effect on the depth estimation. Similar levels of stability in depth estimates in urban environments are reported by other authors, highlighting that, with careful evaluation of electromagnetic wave velocity and the use of hyperbolic fitting, acceptable depth accuracy can be achieved even in heterogeneous subsurface conditions (Conyers 2013, Xie et al. 2013). The presence of characteristic hyperbolic reflections across all GRID sections and free profiles confirms that the detected reflector is spatially and geometrically consistent, which is a key criterion for the reliable identification of linear infrastructure objects. Previous studies have shown that sewer and water pipelines, particularly those of larger diameters, manifest in GPR records as stable hyperbolas with pronounced amplitudes, provided there is sufficient dielectric contrast

between the pipe and the surrounding material (Al-Nuaimy et al. 2000, Kim 2022). The results of this study fully align with these findings. Beyond the technical identification of the pipeline, a critical finding of this study is the significant spatial correlation between the GPR anomalies and the documented water ingress locations within the Kobilja Glava tunnel. Field observations confirm major wastewater leakage in the left tunnel tube between stations 0+460 and 0+510. This area corresponds precisely to the zones in GRID 2 where the radargrams exhibit the strongest signal attenuation and a pronounced "shadowing" effect beneath the pipeline (Fig. 5B). This phenomenon is a direct indicator of high soil saturation caused by the structural failure of the Ø300 mm pipe, which acted as the primary source of uncontrolled fluid infiltration into the tunnel excavation zone. This link between subsurface GPR data and internal tunnel observations provides a robust validation of the interpreted damage zones. The multiple reflections and deeper reflectors observed at certain locations (e.g., GRID 2) can be interpreted as reflections from the bottom of the pipe or as a result of multiple signal bounces under conditions of increased soil moisture. Such phenomena are well documented in the literature and represent common occurrences when surveying areas with infrastructure objects exhibiting pronounced electromagnetic contrasts (Neal 2004, Goodman & Piro 2013). It is important to note that these effects did not compromise the identification of the primary reflector; rather, they further confirmed the presence of the pipeline. The observed vertical oscillations in the pipeline's profile, with depths varying between 1.1 and 1.7 m, do not represent interpretation errors but are a direct consequence of structural deformations. Geotechnical analysis indicates that the tunnel excavation with minimal overburden induced localized ground settlement. Such movements exerted mechanical stress on the joints and the body of the Ø300 mm pipe, leading to the loss of its designed geometry and subsequent structural failure. These deformations explain the irregular alignment of the hyperbola apexes observed in the radargrams, confirming that the GPR method successfully detects not only the presence but also the physical degradation of infrastructural objects. A particular contribution of this study lies in the precise spatial georeferencing of detected reflections within the official coordinate system. In practice, many GPR surveys of underground installations remain limited to relative profiles and local sketches, which significantly reduces their utility for project design and construction. The integration of GPR data with RTK GNSS measurements enabled direct mapping of the sewer pipeline route with centimeter-level accuracy, in line with recommendations from contemporary studies in urban underground mapping (Zembillas 2010, Gabryś & Ortyl 2020). In the context of tunnel structures with minimal overburden, such a level of spatial reliability is especially significant, as it enables engineering decisions to be made based on verified data and substantially reduces the risk of secondary damage during construction. Studies conducted on similar infrastructure projects indicate that the lack of reliable information on the position of existing installations is one of the main causes of unforeseen problems and construction delays (Costello et al. 2007, Vilventhan 2016). While the results demonstrate a high degree of reliability, the limitations of the applied approach must also be emphasized. In this study, the application of a calibrated velocity of 0.09 m/ns (corresponding to a relative dielectric permittivity of $\varepsilon_r \approx 11.1$. proved essential for achieving vertical accuracy. This value, lower than the typical 0.1 m/ns for dry anthropogenic fill, directly reflects the increased soil saturation caused by wastewater leakage. The use of hyperbolic fitting on GRID 2 profiles allowed for an empirical validation of this velocity, ensuring that the calculated reflector depths align with the actual field conditions, despite the complex hydrogeological environment above the tunnel.

Firstly, the estimation of electromagnetic wave velocity is based on the interpretation of hyperbolic reflections, introducing a certain degree of subjectivity. Additionally, local variations in soil moisture and composition can cause changes in dielectric permittivity that cannot always be precisely quantified without additional calibration measurements. Similar limitations are highlighted by other authors, who stress that GPR results in urban environments should always be considered in combination with engineering judgement and, where possible, additional verification methods

(Al-Qadi & Lahouar 2005, Benedetto et al. 2016, Hislop 2016, Rhee et al. 2021, Domitrović et al. 2024). Despite these limitations, the integrated GPR-GNSS approach applied in this study proved to be methodologically robust and practically applicable. The results confirm the initial hypothesis that centimeter-level spatial accuracy in determining the position of sewer installations can be achieved even in the immediate vicinity of tunnel structures. This study therefore aligns with contemporary trends in the development of non-destructive methods for reliable underground infrastructure management and represents a valuable contribution to the application of geophysical methods in engineering practice.

CONCLUSIONS

This study confirms that the integration of GPR with high-precision RTK GNSS provides a robust methodology for the non-destructive mapping of critical underground infrastructure in complex urban environments. By synchronizing GPR scans with network RTK GNSS, we achieved centimeter-level georeferencing accuracy, which proved essential for verifying the spatial position of the sewer pipeline in the absence of reliable cadastral documentation. The research successfully identified structural deformations of the pipeline above the Kobilja Glava tunnel, where recorded depth variations between 1.1 and 1.7 m were interpreted not as measurement uncertainties, but as empirical evidence of ground settlement induced by tunnel excavation. Furthermore, the identification of signal attenuation and the "shadowing" effect provided indirect yet reliable diagnostic indicators of high soil saturation, effectively localizing the areas of wastewater leakage. While these findings provided critical data for the immediate rehabilitation of the site, it is important to emphasize that this research serves as a site-specific case study. The inherent complexities of heterogeneous urban soils suggest that while the GPR-GNSS integration is a powerful risk-mitigation tool, its results should ideally be interpreted alongside broader geotechnical data. Ultimately, this approach demonstrates a clear scientific and practical pathway for protecting utility integrity during major infrastructure projects, reducing the risk of secondary damage and optimizing construction planning.

The author Luka Crnogorac would like to express their sincere gratitude for the support provided by the Ministry of Science, Technological Development, and Innovation of the Republic of Serbia, within the framework of support for scientific research at the University of Belgrade, Faculty of Mining and Geology in Belgrade, under contract number 451-03-34/2026-03/200126.

REFERENCES

Al-Nuaimy W., Huang Y., Nakhkash M., Fang M.T.C., Nguyen V.T. & Eriksen A., 2000. Automatic detection of buried utilities and solid objects with ground-penetrating radar using neural networks and pattern recognition. *Journal of Applied Geophysics*, 43(2–4), 157–165. https://doi.org/10.1016/S0926-9851(99)00055-5.

Al-Qadi I. & Lahouar S., 2005. Measuring layer thicknesses with GPR – theory to practice. *Construction and Building Materials*, 19(10), 763–772. https://doi.org/10.1016/j.conbuildmat.2005.06.005.

Annan A.P., 2005. GPR methods for hydrogeological studies. [in:] Rubin Y. & Hubbard S.S. (eds.), *Hydrogeophysics*, Water Science and Technology Library, 50, Springer, Dordrecht, 185–213. https://doi.org/10.1007/1-4020-3102-5_7.

Bakir H.B., 2017. *Assessment of vertical and horizontal ground penetrating radar resolution for typical models of different targets*. University of Baghdad, College of Science, Department of Geology, Baghdad 2017 [PhD thesis]. https://doi.org/10.13140/RG.2.2.18658.73927.

Barzaghi R., Cazzaniga N.E., Pagliari D. & Pinto L., 2016. Vision-based georeferencing of GPR in urban areas. *Sensors*, 16(1), 132. https://doi.org/10.3390/s16010132.

Bektašević E., Filipović S., Gutić K. & Musa N., 2024. Defining the optimal distance between technological sequences during tunnel excavation in poor rock mass. *e-Zbornik: Electronic Collection of Papers, Faculty of Civil Engineering, University of Mostar*, 14(28), 45–55. https://doi.org/10.47960/2232-9080.2024.28.14.47.

Bektašević E., Filipović S., Gutić K., Hodžić D. & Musa N., 2025a. Analysis of surface deformations during excavation of a small overburden tunnel in weak rock masses. *Journal of the Faculty of Civil Engineering and Architecture*, 40(1), 35–48. https://doi.org/10.62683/ZRGAF40.3.

Bektašević E., Filipović S., Crnogorac L., Gutić K., Požegić Z. & Tokalić R., 2025b. Challenges of tunnel support in low overburden zones in urban areas – case study. *Applied Sciences*, 15(22), 12094. https://doi.org/10.3390/app152212094.

Bektašević E., Filipović S., Hurlov E. & Gutić K., 2025c. Application of a non-destructive method in the analysis of the homogeneity of a concrete foundation in a tunnel structure. *e-Zbornik: Electronic Collection of Papers, Faculty of Civil Engineering, University of Mostar*, 15(30), 71–83. https://doi.org/10.47960/2232-9080.2025.30.15.71.

Benedetto A. & Pajewski L. (eds.), 2015. *Civil Engineering Applications of Ground Penetrating Radar*. Springer, Cham. https://doi.org/10.1007/978-3-319-04813-0.

Benedetto A., Tosti F., Bianchini Ciampoli L. & D'Amico F., 2016. An overview of ground-penetrating radar signal processing techniques for road inspections. *Signal Processing*, 132, 201–217. https://doi.org/10.1016/j.sigpro.2016.05.016.

Bristow C.S. & Jol H.M., 2003. An introduction to ground penetrating radar (GPR) in sediments. [in:] Bristow C.S. & Jol H.M. (eds.), *Ground Penetrating Radar in Sediments*, Geological Society Special Publications, 211, Geological Society, London, 1–7. https://doi.org/10.1144/GSL.SP.2001.211.01.01.

Catapano I., Gennarelli G., Ludeno G., Soldovieri F. & Persico R., 2019. Ground-penetrating radar: Operation principle and data processing. [in:] Webster J.G. (ed.), *Wiley Encyclopedia of Electrical and Electronics Engineering*, Wiley, Hoboken, NJ, 1–23. https://doi.org/10.1002/047134608x.w8383.

Conyers L.B., 2013. *Ground-Penetrating Radar for Archaeology* (3rd ed.). AltaMira Press, Lanham.

Costello S.B., Chapman D.N., Rogers C.D.F. & Metje N., 2007. Underground asset location and condition assessment technologies. *Tunnelling and Underground Space Technology*, 22(5–6), 524–542. https://doi.org/10.1016/j.tust.2007.06.001.

Daniels D.J., 2004. *Ground Penetrating Radar* (2nd ed.). IET Radar, Sonar and Navigation Series, 15, The Institution of Engineering and Technology, London.

Davis J.L. & Annan A.P., 1989. Ground-penetrating radar for high-resolution mapping of soil and rock stratigraphy. *Geophysical Prospecting*, 37(5), 531–551. https://doi.org/10.1111/j.1365-2478.1989.tb02221.x.

Domitrović J., Dukić M., Bezina Š., Stančerić I. & Rukavina T., 2024. Reliability of GPR data interpretation methods for determining the thickness of asphalt layer. [in:] Lakušić S. (ed.), *Road and Rail Infrastructure VIII: Proceedings of the 8th International Conference on Road and Rail Infrastructures – CETRA 2024, 15–17 May 2024, Cavtat, Croatia,* University of Zagreb, Zagreb, 717–723. https://doi.org/10.5592/CO/CETRA.2024.1652.

Filipović S., Bektašević E., Gutić K., Musa N. & Sakić N., 2025. Research on the phenomenon of increasing borehole diameter at the installation of rod anchors in marl using wet technology compared to dry drilling procedure. *Global Journal of Engineering and Technology Advances*, 22(2), 001–014. https://doi.org/10.30574/gjeta.2025.22.2.0019.

Gabryś M. & Ortyl Ł., 2020. Georeferencing of multi-channel GPR – accuracy and efficiency of mapping of underground utility networks. *Remote Sensing*, 12(18), 2945. https://doi.org/10.3390/rs12182945.

Ghanbari S., Hafizi M. K., Bano M., Ebrahimi A. & Hosseinzadeh N., 2022. An enhanced GPR-based data processing approach for detecting subsurface utilities in urban distribution networks. *Journal of Applied Geophysics*, 207, 104831. https://doi.org/10.1016/j.jappgeo.2022.104831.

Goodman D., 1994. Ground-penetrating radar simulation in engineering and archaeology. *Geophysics*, 59(2), 224–232. https://doi.org/10.1190/1.1443584.

Goodman D. & Piro S., 2013. GPR *Remote Sensing in Archaeology*. Springer, Berlin–Heidelberg. https://doi.org/10.1007/978-3-642-31857-3.

He T. & Shang H., 2020. Direct-wave denoising of low-frequency ground-penetrating radar in open pits based on empirical curvelet transform. *Near Surface Geophysics*, 18(2), 451–462. https://doi.org/10.1002/nsg.12095.

Hislop G., 2016. Limitations of characterizing layered earth with off-ground GPR. *Journal of Geophysics and Engineering*, 13(2), S1–S8. https://doi.org/10.1088/1742-2132/13/2/S1.

Huurne R.B.A., ter, Olde Scholtenhuis L.L., Dorée A.G., 2024. Ground penetrating radar at work: A realistic perspective on utility surveying in the Netherlands through a comprehensive ground-truth dataset. *Data in Brief*, 54, 110329. https://doi.org/10.1016/j.dib.2024.110329.

ImpulseRadar GPR Team., 2021. *GPR antenna frequency vs. depth penetration vs. resolution*. ImpulseRadar. https://impulseradargpr.com/gpr-antenna-frequency-vs-depth-penetration-vs-resolution/ [access: 4.07.2025].

Jol H.M. (ed.), 2009. *Ground Penetrating Radar: Theory and Applications*. Elsevier.

Jol H.M. & Bristow C.S., 2006. Ground-penetrating radar profile spacing and orientation for subsurface resolution of linear features. *Geophysical Prospecting*, 54(1), 63–72. https://doi.org/10.1111/j.1365-2478.2006.00516.x.

Kim S.S., 2022. Assessment of pavement structural conditions using a ground-penetrating radar. *Engineering Proceedings*, 17(1), 1. https://doi.org/10.3390/engproc2022017001.

Kruk J., van der, Slob E.C. & Fokkema J.T., 1998. Background of ground penetrating radar measurements. *Geologie en Mijnbouw*, 77(2), 177–188.

Luo T.X.H. & Lai W.W.L., 2020. GPR pattern recognition of shallow subsurface air voids. *Tunnelling and Underground Space Technology*, 99, 103355. https://doi.org/10.1016/j.tust.2020.103355.

Massarelli C., Campanale C. & Uricchio V.F., 2021. Ground penetrating radar as a functional tool to outline the presence of buried waste: A case study in South Italy. *Sustainability*, 13(7), 3805. https://doi.org/10.3390/su13073805.

Neal A., 2004. Ground penetrating radar and its use in sedimentology: Principle, problem and progress. *Earth-Science Reviews*, 66, 261–330. https://doi.org/10.1016/j.earscirev.2004.01.004.

Pajewski L., Benedetto A., Loizos A., Slob E., Tosti F. & Roberts S., 2014. Civil engineering applications of ground penetrating radar: First-year activities and results. *Geophysical Research Abstracts*, 16, EGU2014_16933.

Poluha B., Porsani J.L., Almeida E.R., dos Santos V.R.N. & Allen S.J., 2017. Depth estimates of buried utility systems using the GPR method: Studies at the IAG/USP Geophysics Test Site. *International Journal of Geosciences*, 8(5), 726–742. https://doi.org/10.4236/ijg.2017.85040.

Rangole A., De S., Kuchekar N. & Bazil Raj A.A., 2024. A comprehensive review of ground penetrating radar: Techniques, applications and future directions. *International Journal of Engineering Research and Reviews*, 12(3), 30–53. https://doi.org/10.5281/zenodo.13842586.

Rasol M., Perez-Gracia V. & Santos-Assunçao S., 2021. *Development of new GPR methodologies for soil and cement concrete pavement assessment*. Universitat Politècnica de Catalunya, Barcelona [PhD thesis]. https://doi.org/10.13140/RG.2.2.32976.74242.

Rasol M., Perez-Gracia V., Fernandes F., Pais J., Santos-Assunçao S. & Roberts S., 2022. Ground penetrating radar system: Principles. [in:] D'Amico S. & Venuti V. (eds.), *Handbook of Cultural Heritage Analysis*, Springer, Cham, 705–738. https://doi.org/10.1007/978-3-030-60016-7_25.

Reynolds J.M., 2011. *An Introduction to Applied and Environmental Geophysics* (2nd ed.). Wiley-Blackwell.

Rhee J.-Y., Park K.-T., Cho J.-W. & Lee S.-Y., 2021. A study of the application and the limitations of GPR investigation on underground survey of the Korean expressways. *Remote Sensing*, 13(9), 1805. https://doi.org/10.3390/rs13091805.

Robinson M., Bristow C., McKinley J. & Ruffell A., 2013. Ground-penetrating radar guidelines: Survey design and implementation. *Geomorphological Techniques*, 1(5.5). https://pure.qub.ac.uk/en/publications/431bd8bd-279f-4d95-8434-84b38c63a9d5.

Sukhenko A., Meirambekuly N., Syzdykov A., Mukhamedgali A. & Mellatova Y., 2025. GNSS for high-precision and reliable positioning: A review of correction techniques and system architectures. *Applied Sciences*, 15(22), 12304. https://doi.org/10.3390/app152212304.

Travassos X., Ida N., Avila S.L. & Adriano R., 2018. A review of ground penetrating radar antenna design and optimization. *Journal of Microwaves, Optoelectronics and Electromagnetic Applications*, 17(3), 385. https://doi.org/10.1590/2179-10742018v17i31321.

Vilventhan A., 2016. Interrelationships of factors causing delays in the relocation of utilities: A cognitive mapping approach. *Engineering, Construction and Architectural Management*, 23(3), 349–368. https://doi.org/10.1108/ECAM-10-2014-0127.

Wang S., Liu G., Jing G., Feng Q., Liu H. & Guo Y., 2022. State-of-the-art review of ground penetrating radar (GPR) applications for railway ballast inspection. *Sensors*, 22(7), 2450. https://doi.org/10.3390/s22072450.

Xie X., Zeng C. & Wang Z., 2013. GPR signal enhancement using band-pass and K–L filtering: A case study for the evaluation of grout in a shielded tunnel. *Journal of Geophysics and Engineering*, 10(3), 034003. https://doi.org/10.1088/1742-2132/10/3/034003.

Zembillas N., 2010. Subsurface utility engineering: A proven solution. [in:] *FIG Congress 2010: Facing the Challenges – Building the Capacity: Sydney, Australia, 11–16 April 2010*, International Federation of Surveyors, 1–9. https://www.fig.net/resources/proceedings/fig_proceedings/fig2010/papers/fs04g/fs04g_zembillas_4659.pdf.

Zhang J., Hu Q., Zhou Y., Zhao P. & Duan X., 2024. A multi-level robust positioning method for three-dimensional ground penetrating radar (3D GPR) road underground imaging in dense urban areas. *Remote Sensing*, 16(9), 1559 https://doi.org/10.3390/rs16091559.

Zhou Y., Wong P.T. W., Li Y., Lai W.W.L. & Wang J., 2026. Enhancing multichannel ground penetrating radar (MCGPR) positioning using cross-channel data. *Measurement*, 257(Part B), 118715. https://doi.org/10.1016/j.measurement.2025.118715.